LIU PENG
and
YUE JIANHUA

Dynamic monitor of coal seam floor limestone water grouting based on TL-ERT

This paper takes the characteristics of timing data from Time-Lapse Electrical Resistivity Tomography monitor as basis, introduces the Kalman filter technique for a recursive process on the natural electric field data of monitor samples to achieve the timing inversion on monitor data. The dynamic surveillance can be carried out on how the spatial and temporal changes, such as groundwater movement law, water inrush prediction, quarry and mining surveillance. Time-lapse surveillance in a small area of the seam roadway on a short time scale has further proved that the Kalman algorithm has good effect on the inversion process of monitor data. The monitor data inversion interpretation in the natural electric field characterizes the variation of the electrical properties of the floor before and after grouting. The internal correlation between water movement and grouting change is thereby built up. These features attributes TL- Early to playing a good effect in the early-warning of floor water inrush.

Keywords: Time-shift resistivity tomography, Kalman filter technique, dynamic monitor.

1. Introduction

Today, the deep exploitation in our coal mines gets more widespread, especially in some old mines in the east of China, where they face the threat from a main type of the floor limestone water disaster. To ensure the safe backstopping of working faces, it is required to carry out the grouting reinforcement on floor limestone water. We must determine in advance whether there are some possible floor cracks and the aqueducts, if so, the exact locations shall be given for the borehole blockage.

Time-Lapse Electrical Resistivity Tomography (TL-ERT) [1-10] incorporates the time-series data inversion whereby to provide a direct observation on the dynamical variation in subsurface electrical property and further know about the subsurface-hydrogeological characteristics and how they change. TL-ERT is widely used in the fields of the hydrogeological permeability coefficient prediction

Messrs. Liu Peng and Yue Jianhua, College of Resource & Geosciences, China University of Mining & Technology, Xuzhou 221008, Yankuang Donghua Construction Co., Ltd., Zoucheng 273500, China

(Hayleyetal.,2009; Kurasetal.,2009), salt water encroachment (Martorana et al., 2014). As an optimal estimation technique, Kalman is prevalent in the dynamic system parameter estimation. Lehikoinen et al. (2009, 2010) implemented a dynamic estimation on the geoelectric model parameters by applying the Kalman algorithm [11-16] in the DC resistivity monitor data process. The Kalman presents a good temporal regularization effect when performing time-series data inversion and model estimation. This paper explores the application effect of TL-ERT with an experiment that Kalman is introduced to process the monitor data on the natural electric field and by taking the time-series inversion of dynamic monitor data about grouting on working face 11605, Daizhuang Coal Mine, Zibo Mining Group as the study case.

2. Geoelectricity model

2.1 DYNAMIC MODEL

In the process of grouting in the floor, the hydraulic layers of the subfloor aquifer continuously change over time. The continuous change model is monitored with the dynamic model $\hat{N}$ represented by the discrete model which corresponds to all monitoring time points.

$$\Box N = [N_I \dots N_i \dots]^T \qquad \dots 1$$

Where, N_i is the model corresponding to the time i.

In saturated porous media, the parameters such as medium porosity ϕ, water saturation S_W, and saturation coefficientnare the constants. Archie formula, used for calculating the conductivity of porous media, can be simplified to be

$$\sigma(S) = k_a \sigma_w \left(k_a = \phi^b s_w^n \right) \qquad \dots 2$$

That is, the conductivity distribution of the medium depends on that of the pore water. If the conductivity of the pore water and the ion concentration are regarded as a linearity (coefficient k_c), formula (2) can be rewritten as

$$\sigma(S) = k_a k_c S \qquad \dots 3$$

It follows that the change of the hydraulic parameters of the subfloor aquifer is equivalent to that of the conductivity distribution of the whole system, and it is true for the dynamic changes of the model statuses at the current time k and at

the previous time $k-1$ as follows

$$\sigma(S)_k = H_k \, \sigma(S)_{k-1} + w_k \qquad \text{... 4}$$

Simplified as

$$M_k = HM_{k-1} + w_k \qquad \text{... 5}$$

Where H is the status evolution operator expressed by Eqs. (2) and (3); M_k is the model status characterized by the ion concentration; w_k is the process noise caused by various factors.

2.2 INVERSION ALGORITHM

The monitor data $\hat{D}$ that the dynamic model corresponds to is expressed as

$$\hat{D} = [d_1 \dots d_i]^T \qquad \text{... 6}$$

Where d_i is the monitor data corresponding to the time i.

Based on the conductivity distribution [observation data in Eq. (6)], the current density of the streaming potential in the porous medium can be available by forward computation, that is,

$$Z_k = FN_k + v_k \qquad \text{... 7}$$

Where, Z_k is the observation of the model N_k in current time k; F is the status observation operator, and the model space status is mapped into the observation data set. v_k is the observation noise.

The Kalman filter of dynamic process is built by the model status process Eqs. (5) and observation model (7). The filtering process can calculate the current status estimation by using the status estimation of the previous time and the current observation data, namely that the recursion process undergoes two phases, i.e. "prediction" and "correction". The "prediction" phase can be expressed as

$$\hat{N}_{K/K-1} = H\hat{N}_{K-1|K-1} \qquad \text{... 8}$$

The "correction" phase can be expressed as

$$\hat{N}_{K/K} = \hat{N}_{K/K-1} + K_K (Z_K - F\hat{N}_{K|K-1}) \qquad \text{... 9}$$

In the process of the filter correction, the a posteriori estimation status is derived from the a priori estimation status plus the Kalman gain-weighted correction. This method can transfer the previous observations to the current time in order to increase the observational data volume. With the continuous addition of observation data, the model status to be solved can be constantly corrected and more approach to the real model, so that a real-time inversion of time series observation data are achieved.

3. Inversion test

3.1 HYDROGEOLOGICAL CONDITION

In the scope of this working face, the thickness of Shixia limestone aquifers is 5.20m or so. The development of karst fissures is uneven. The Shixia limestone L10-4 ground observation conducted on August 25, 2009 shows that the average water level elevation of the hole is about -64.637m (the highest water level in the recent three year), q = 0.00157~0.1857 l/sm, $K = 0.3551~5.1686$ m/d, the salinity 1.9144~2.3885 g/l, and the water quality belongs to $SO_4 \cdot HCO_3$–Ca·K+Na type, i.e. the moderate water-rich aquifers with better conditions. This aquifer is a nether roof of coal [16].

In work face 11605, there is a normal fault DF9 along the elements of attitude: 76°, leaning to 166°, at a dipping angle of 73°, with a fall of 0~5.0m.

In the face 11605, there are a row of non-polarized electrodes, 85 in total, arranged on the coal seam floor at the spacing of 10m; a measuring line is about 850m long. The multi-channel electrical instrument measures up these electrodes to monitor the change in the natural electric field of floor.

3.2 PHYSICAL MEASUREMENT DATA

The algorithm is tested with actual measurements of the natural electric field time-series data before and after floor limestone water grunting on work face 11605 in order to determine whether the physical model and the inversion algorithm play a good effect. In the process of floor grouting, the change in the natural electric field is monitored and recorded. The electrodes are arranged at an interval of 10m and the grouting bore is located in the middle part of the roadway.

Monitor data at 10 o'clock every day will be taken as sample data to draw the potential values measured for each electrode, as shown in Fig.1 (a), (b), (c), (d), (e) and (f) correspond to the curves of the natural electric field data sampled as the function of certain times from D1 to D6, respectively.

Along with the grunting, the electrode potential in the strata near the borehole changes significantly, but a little in the strata far away from the borehole. When sampling in Day 2, the natural potential value of electrode reaches the peak, and then declines slowly, while remains stable on Day 5.

The time series inversion is carried out on the collected natural electric field data. As shown in Fig.2 (a), (b), (c), (d), (e) and (f) correspond to the results of the inversion at 10 a.m., Day 1, at 10 a.m. Day 2, and at 10 a.m. Day 6, respectively. The inversion results from the monitor data of the natural electric field of coal seam floor show that the apparent resistivity in vertical direction changes significantly in the wake of grouting. With gradually increasing of apparent resistivity, the aqueous area gradually narrows, which indicates that the effluent point of floor has been effectively controlled. The observations roughly coincides with the inversion results, which further suggests that the time-series inversion can be effectively applied to the measured data of the natural electric field so as to reconstruct the dynamic process.
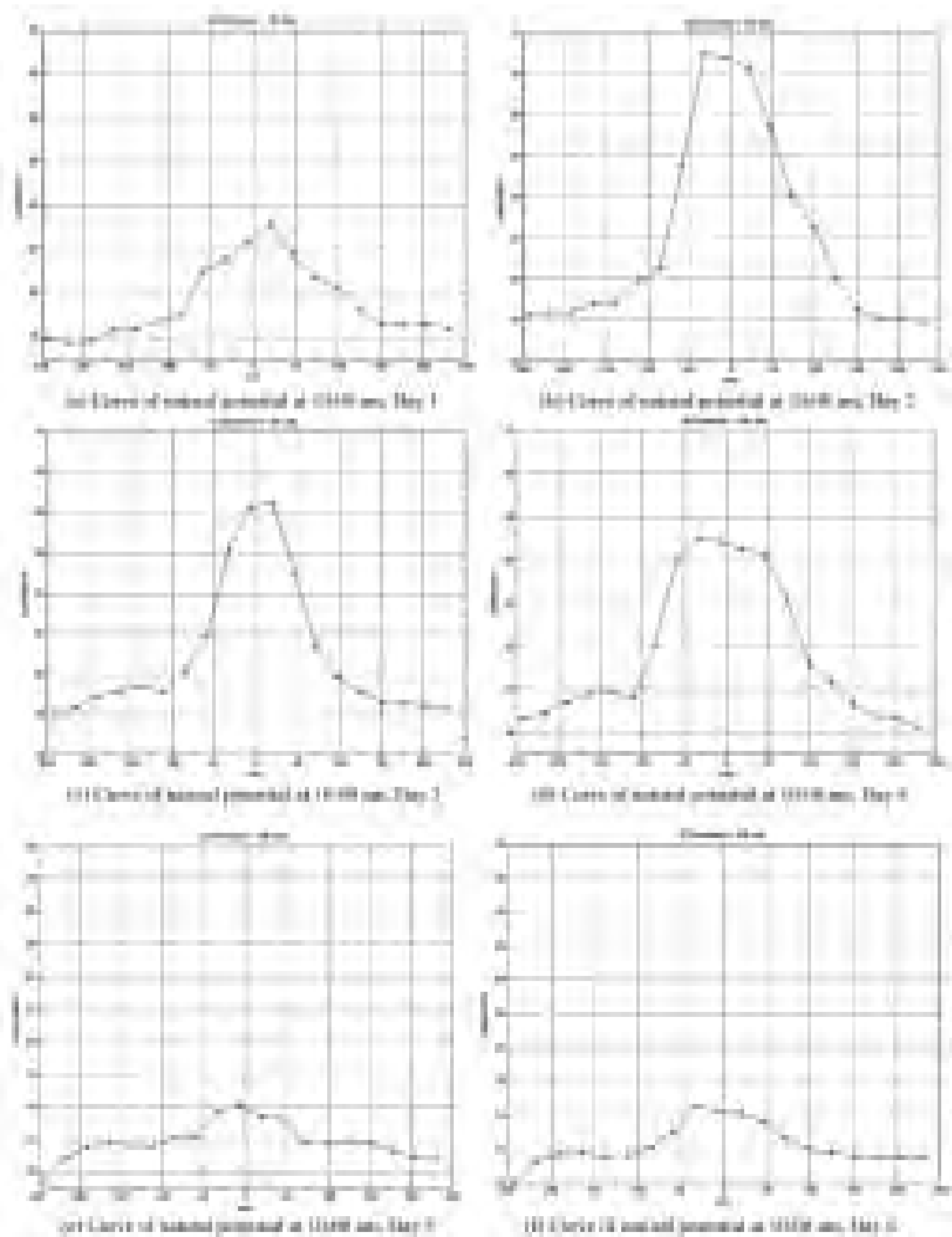
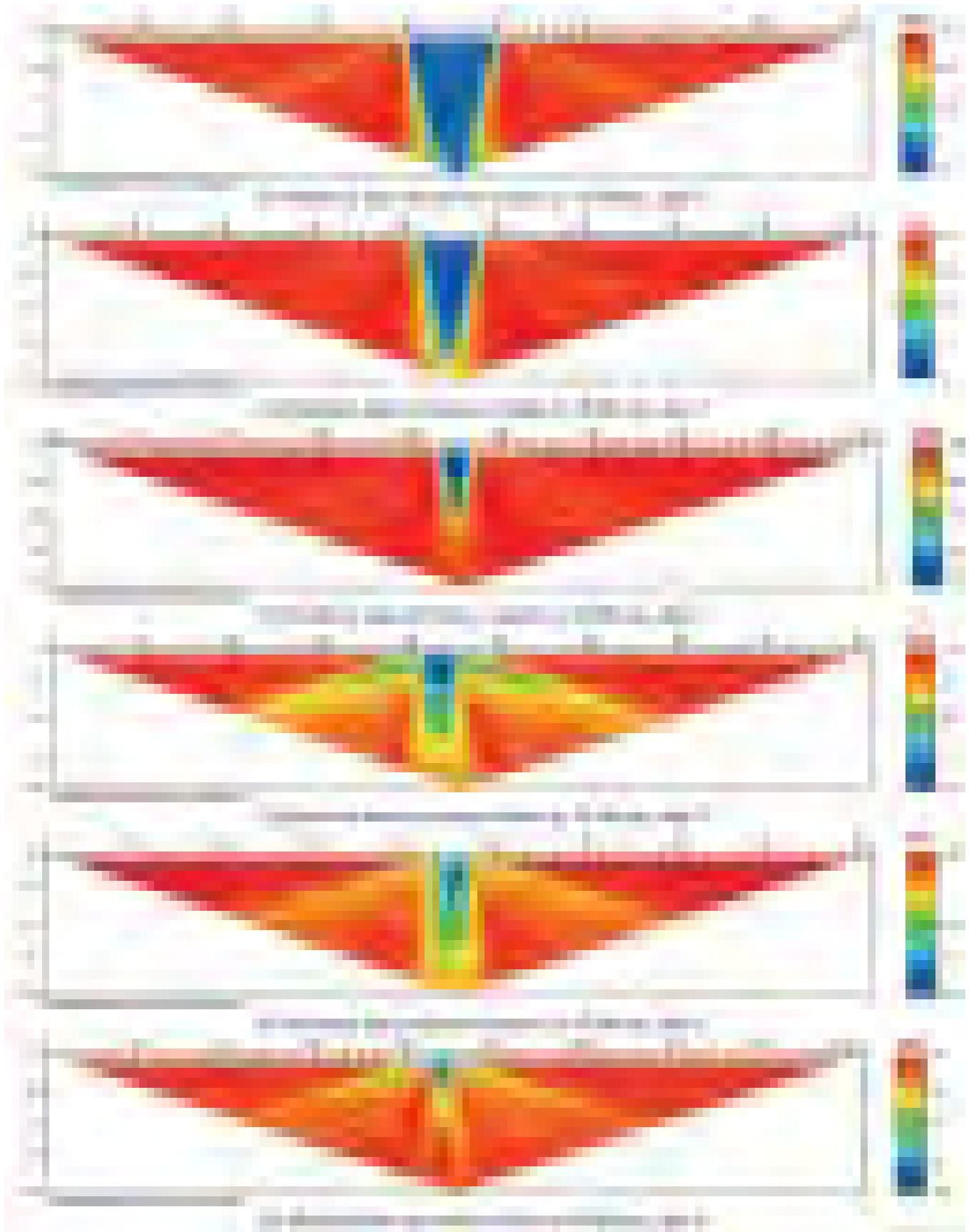Fig.1 Curve of the natural electric field monitor data in coal seam floor

Fig.2 Monitor data inversion results in coal seam floor

4. Conclusion

Based on the characteristics of timing data from Time-lapse Electrical Resistivity Tomography monitor, the Kalman filter technique is adopted to perform a recursive process on the natural electric field data of monitor samples in order to achieve timing inversion on monitor data. The dynamic surveillance can be carried out on how the spatial and temporal changes, such as groundwater movement law, water inrush prediction, quarry and mining surveillance. Time-lapse surveillance in a small area of the seam roadway on a short time scale has further proved that the Kalman algorithm has good effect on the inversion process of monitor data. The monitor data inversion interpretation in the natural electric field characterizes the variation of the electrical properties of the floor before and after grouting. The internal correlation between water movement and grouting change is thereby built up. These features attributes TL- early to playing a good effect in the early-warning of floor water inrush.

References

[1] Labrecque, D.J., Yang, X. (2001): "Difference inversion of ERT data: a fast inversion method for 3-D in situ monitoring," *Journal of Environmental and Engineering Geophysics,* no. 5, pp. 83-90.

[2] Legaz, A., Vandemeulebrouck, J., Revil, A., Kemna, A., Hurst, A.W., Reeves, R., Papasin, R., (2009): "Acase study of resistivity and self-potential signatures of hydrothermal instabilities, Inferno Crater Lake, Waimangu, New Zealand," *Geophysical Research Letters*, vol. 36, pp. L12306.

[3] Leroux, V., DAHLIN, T., (2006): "Time-lapse resistivity investigations for imaging saltwater transport in glaciofluvial deposits," *Environmental Geology*, vol. 49, no. 3, pp. 347-358.

[4] Looms, M.C., Jensen, K.H., Binley, A., Nielsen, L., (2008): "Monitoring unsaturated flowand transport using cross-borehole geophysical methods," *Vadose Zone Journal*, no. 7, pp. 227-237.

[5] Miller, C.R., Routh, P.S., Brosten, T.R., Mcnamara, J.P., (2008): "Application of time-lapse ERT imaging to watershed characterization," *Geophysics*, vol. 73, pp. G7-G17.

[6] Müller, K., Vanderborght, J., Englert, A., Kemna, A., Huisman, J.A., Rings, J., Vereecken, H. (2010): "Imaging and characterization of solute transport during two tracer tests in a shallow aquifer using electrical resistivity tomography and multilevel groundwater samplers," *Water Resources Research*, no. 46, pp. W03502.

[7] Nguyen, F., Kemna, A., Antonsson, A., Engesgaard, P., Kuras, O., Ogilvy, R., Gisbert, J., Jorreto, S., Pulido-bossch, A. (2009): "Characterization of seawater intrusion using 2D electrical imaging," *Near-Surface Geophysics*, vol. 7, no. 5-6, pp. 377-390.

[8] Nimmer, R.E., Osiensky, J.L., Binley, A.M., Sprenke, K.F., Williams, B.C. (2007): "Electrical resistivity imaging of conductive plume dilution in fractured rock," *Hydrogeology Journal*, no. 5, pp. 877-890.

[9] Ogilvy, R.D., Kuras, O., Meldrum, P.I., Wilkinson, P.B., Chambers, J.E., Sen, M., Gisbert, J., Jorreto, S., Frances, I., Pulido-bosch, A., Tsourlos, P. (2009): "Automated time-Lapse Electrical Resistivity Tomography (ALERT) for monitoring Coastal Aquifers," *Near Surface Geophysics*, vol. 7, no. 5-6, pp. 367-375.

[10] Oldenborger, G.A., Knoll, M.D., Routh, P.S., Labrecque, D.J. (2007): "Time-lapse ERT monitoring of an injection/withdrawal experiment in a shallow unconfined aquifer," *Geophysics*, vol. 72, no. 4, pp. F177-F187.

[11] Park, S. (1998): "Fluid migration in the vadose zone from 3-D inversion of resistivity monitoring data," *Geophysics*, vol. 63, no. 1, pp. 41-51.

[12] Ramirez, A., Daily, W., Labrecque, D.J., Owen, E. and Chesnut, D. (1993): "Monitoring an underground steam injection process using electrical resistance tomography," *Water Resources Research*, vol. 29, pp. 73-87.

[13] Singha, K., Gorelick, S.M. (2005): "Saline tracer visualized with electrical resistivity tomography:field scale spatial moment analysis," *Water Resour. Res.*, vol. 41, pp. W05023.

[14] Slater, L., Binley, A.M., Versteeg, R., Cassiani, G., Birken, R., Sandleberg, S. (2002): "A 3D ERT study of solute transport in a large experimental tank," *Journal of Applied Geophysics*, vol. 49, no. 4, pp. 211–229.

[15] Zhang, Y., Ghodrati, A., Brooks, D.H. (2005): "An analytical comparison of three spatiotemporal regularization methods for dynamic linear inverse problems in a common statistical framework," *Inverse Problems*, vol. 21, pp. 357-382.

[16] Loke, M. H., Chambers, J. E., Rucker, D. F., Kuras,O., and Wilkinson, P. B. (2013): "Recent developments in the direct-current geoelectrical imaging method," *Journal of Applied Geophysics*, vol. 95, no. 8, pp. 135–156.